

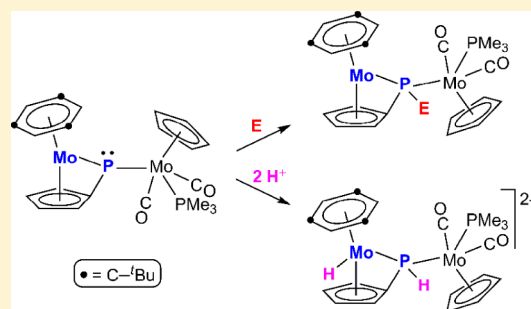
Electronic Structure and Multisite Basicity of the Pyramidal Phosphinidene-Bridged Dimolybdenum Complex $[\text{Mo}_2(\eta^5\text{-C}_5\text{H}_5)(\mu\text{-}\kappa^1:\kappa^1,\eta^5\text{-PC}_5\text{H}_4)(\eta^6\text{-C}_6\text{H}_3\text{tBu}_3)(\text{CO})_2(\text{PMe}_3)]$

Isabel G. Albuérne, M. Angeles Alvarez, M. Esther García, Daniel García-Vivó,* and Miguel A. Ruiz*

Departamento de Química Orgánica e Inorgánica/IUQOEM, Universidad de Oviedo, E-33071 Oviedo, Spain

S Supporting Information

ABSTRACT: The title phosphinidene complex could be sequentially protonated with $\text{HBF}_4\cdot\text{OEt}_2$ or $[\text{H}(\text{OEt}_2)_2](\text{BAR}'_4)$ to give the phosphido-bridged derivatives $[\text{Mo}_2\text{Cp}(\mu\text{-}\kappa^1:\kappa^1,\eta^5\text{-HPC}_5\text{H}_4)(\eta^6\text{-HMes}^*)(\text{CO})_2(\text{PMe}_3)]\text{X}$ and then the hydrides $[\text{Mo}_2\text{Cp}(\text{H})(\mu\text{-}\kappa^1:\kappa^1,\eta^5\text{-HPC}_5\text{H}_4)(\eta^6\text{-HMes}^*)(\text{CO})_2(\text{PMe}_3)]\text{X}_2$ ($\text{X} = \text{BF}_4, \text{BAR}'_4; \text{Ar}' = 3,5\text{-C}_6\text{H}_3(\text{CF}_3)_2; \text{Mes}^* = 2,4,6\text{-C}_6\text{H}_2\text{tBu}_3$). Density functional theory (DFT) calculations revealed that the most favored site for initial electrophilic attack is the metallocene Mo atom, but attachment of the electrophile to the phosphinidene P atom gives more stable products. This was in agreement with all other reactions investigated, which invariably involved the attachment of the added electrophile at the P site. Thus, the title compound reacted with S_8 at 223 K to give the thiophosphinidene-bridged complex $[\text{Mo}_2\text{Cp}\{\mu\text{-}\kappa^1:\kappa^1,\eta^5\text{-P}(\text{S})\text{C}_5\text{H}_4\}(\eta^6\text{-HMes}^*)(\text{CO})_2(\text{PMe}_3)]$, a poorly stable molecule which reacted with MeI at room temperature to give the corresponding thiolatophosphido derivative, isolated as $[\text{Mo}_2\text{Cp}\{\mu\text{-}\kappa^1:\kappa^1,\eta^5\text{-P}(\text{SMe})\text{C}_5\text{H}_4\}(\eta^6\text{-HMes}^*)(\text{CO})_2(\text{PMe}_3)](\text{BAR}'_4)$ ($\text{P-S} = 2.128(4) \text{ \AA}$) after anion exchange with $\text{Na}(\text{BAR}'_4)$. Reaction of the title compound with MeI proceeded smoothly to give the corresponding methylphosphido derivative, isolated analogously as $[\text{Mo}_2\text{Cp}\{\mu\text{-}\kappa^1:\kappa^1,\eta^5\text{-P}(\text{Me})\text{C}_5\text{H}_4\}(\eta^6\text{-HMes}^*)(\text{CO})_2(\text{PMe}_3)](\text{BAR}'_4)$. The related complex $[\text{Mo}_2\text{Cp}\{\mu\text{-}\kappa^1:\kappa^1,\eta^5\text{-P}(\text{Me})\text{C}_5\text{H}_4\}(\eta^6\text{-HMes}^*)(\text{CO})_2(\text{PMe}_2\text{Ph})](\text{BAR}'_4)$ ($\text{P-C}(\text{Me}) = 1.841(5) \text{ \AA}$) could be prepared analogously from the neutral precursor $[\text{Mo}_2\text{Cp}\{\mu\text{-}\kappa^1:\kappa^1,\eta^5\text{-PC}_5\text{H}_4\}(\eta^6\text{-HMes}^*)(\text{CO})_2(\text{PMe}_2\text{Ph})]$. In contrast, reaction of the title complex with ethylene sulfide involved opening of the C_2S ring and formation of new P–C and Mo–S bonds ($1.886(7)$ and $2.493(2) \text{ \AA}$, respectively), with displacement of the PMe_3 ligand, to give the phosphido–thiolato complex $[\text{Mo}_2\text{Cp}\{\mu\text{-}\kappa^2_{\text{P,S}}:\kappa^1_{\text{P}},\eta^5\text{-P}(\text{C}_2\text{H}_4\text{S})\text{C}_5\text{H}_4\}(\eta^6\text{-HMes}^*)(\text{CO})_2]$. All these derivatives of the title complex displayed an unusual trigonal pyramidal-like environment around the bridging P atom, with the added electrophile placed in the Mo_2P plane as a result of the directionality of the relevant frontier orbital of the phosphinidene complex, according to DFT calculations.

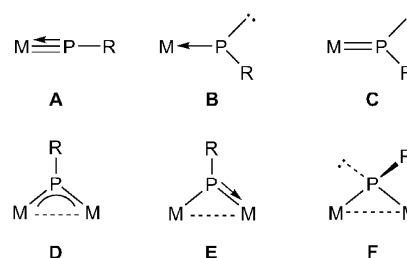


INTRODUCTION

The chemistry of transition metal complexes bearing the multifaceted phosphinidene ligand (PR) continues to be an active area of research within the inorganic chemistry realm.¹ Most of the work in this area, however, has been historically focused on the reactivity of mononuclear complexes, particularly those having bent-terminal ligands (**B** and **C** in Chart 1), much stimulated by their analogy with the corresponding carbene complexes and the possibility of their use as precursors for novel organophosphorus molecules.² When bound to two metal centers, the phosphinidene ligand still retains a considerable chemical potential derived from the presence of multiple M–P bonding or lone electron pairs in any of its possible coordination modes (**D** to **F**), yet the chemistry of binuclear, phosphinidene-bridged complexes has been comparatively far less explored than that of their mononuclear counterparts.^{3–6}

Among the phosphinidene-bridged complexes, those having a pyramidal ligand (type **F**) are expected to display a strongly nucleophilic behavior located at the P site, although our

Chart 1



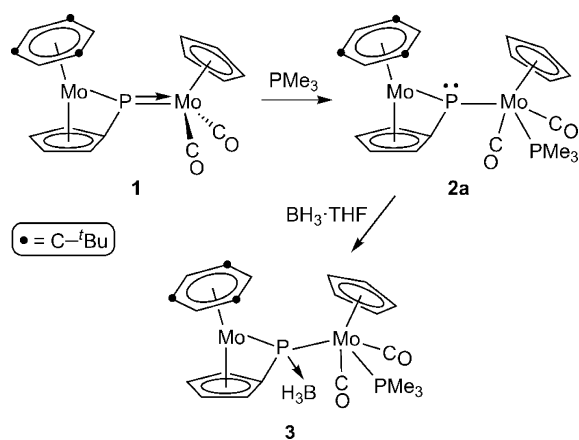
extensive work on diiron complexes of type $[\text{Fe}_2\text{Cp}_2(\mu\text{-PR})(\mu\text{-CO})(\text{CO})_2]$ has revealed that the metal fragments might be also involved in reactions of these complexes with different electrophiles, thus leading to unexpected outcomes.⁵ In this

Received: July 9, 2015

Published: October 8, 2015

context, it is surprising that very little is known so far on the chemistry of group 6 metal complexes of type F. Some time ago, Cowley et al. reported the formation of the bis-(phosphinidene) dimolybdenum complex $[\text{Mo}_2\text{Cp}_2(\mu\text{-PR})_2(\text{CO})_4]$ [$\text{R} = \text{CH}(\text{SiMe}_3)_2$], a poorly characterized molecule stabilized by bulky substituents at phosphorus, but its chemistry was not explored.⁷ Later on, we found that some photochemical reactions of the type D phosphinidene complex $[\text{Mo}_2\text{Cp}_2(\mu\text{-PMes}^*)(\text{CO})_4]$ [$\text{Mes}^* = 2,4,6\text{-C}_6\text{H}_2\text{Bu}_3$] could be understood by assuming the participation of a highly reactive excited state with a geometry of type F able to induce, for instance, intramolecular cleavage in a methyl C–H bond to eventually yield the hydride isomer $[\text{Mo}_2\text{Cp}_2(\mu\text{-H})\{\mu\text{-P}(\text{CH}_2\text{CMe}_2)_2\text{C}_6\text{H}_2\text{Bu}_2\}(\text{CO})_4]$.⁸ We also note that Pikies and co-workers reported the formation of tiny amounts of the pyramidal phosphinidene tungsten complex $[\text{W}_2\text{Cp}_2(\mu\text{-PC}_5\text{H}_4)_2]$,⁹ but obviously its chemistry could not be explored either. Recently, while studying reactions of the type E phosphinidene complex $[\text{Mo}_2\text{Cp}(\mu\text{-}\kappa^1:\kappa^1,\eta^5\text{-PC}_5\text{H}_4)(\eta^6\text{-HMes}^*)(\text{CO})_2]$ (**1**) toward alkynes and olefins in the presence of CO and CNR ligands (L),^{4,10} we came to the conclusion that these reactions actually proceed through undetectable intermediate species of type $[\text{Mo}_2\text{Cp}(\mu\text{-}\kappa^1:\kappa^1,\eta^5\text{-PC}_5\text{H}_4)(\eta^6\text{-HMes}^*)(\text{CO})_2\text{L}]$ resulting from ligand addition to complex **1** and pyramidalization of the P atom, which then becomes nucleophilic enough to attack an external alkyne or alkene molecule. The low stability of such pyramidal intermediates was independently established by analyzing the reaction of **1** with CO in the absence of any further reagent, which then leads to a mixture of the diphosphanediyl complex $[\text{Mo}_2\{\mu\text{-}\kappa^1,\eta^5\text{-}\kappa^1,\eta^5\text{-}(\text{C}_5\text{H}_4)\text{PP}(\text{C}_5\text{H}_4)(\eta^6\text{-HMes}^*)_2\}]$ and $[\text{Mo}_2\text{Cp}_2(\text{CO})_6]$, these products following from homolytic P–Mo bond cleavage in the (undetected) pyramidal intermediate $[\text{Mo}_2\text{Cp}(\mu\text{-}\kappa^1:\kappa^1,\eta^5\text{-PC}_5\text{H}_4)(\eta^6\text{-HMes}^*)(\text{CO})_3]$.¹¹ We afterward found that the use of a stronger electron donor such as PMe_3 improved the stability of this sort of pyramidal intermediate. Indeed compound **1** reacted with PMe_3 instantaneously at room temperature to yield a thermally stable, though quite air-sensitive, pyramidal derivative $[\text{Mo}_2\text{Cp}(\mu\text{-}\kappa^1:\kappa^1,\eta^5\text{-PC}_5\text{H}_4)(\eta^6\text{-HMes}^*)(\text{CO})_2(\text{PMe}_3)]$ (**2a**) (Scheme 1). Our preliminary studies then pointed to a P-based nucleophilic behavior of this molecule, able to form the expected borane adduct $[\text{Mo}_2\text{Cp}\{\mu\text{-}\kappa^1:\kappa^1,\eta^5\text{-P}(\text{BH}_3)\text{C}_5\text{H}_4\}(\eta^6\text{-HMes}^*)(\text{CO})_2(\text{PMe}_3)]$ (**3**), but also able to induce unexpected rearrangements in the electrophile being added, as found in its reaction with maleic anhydride.¹²

Scheme 1

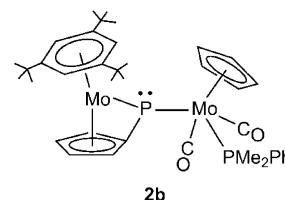


We then decided to explore in detail the chemistry of this pyramidal phosphinidene complex, which is the purpose of the present research. In this paper we analyze the geometric and electronic structure of compound **2a** and its reactions with Brønsted acids, chalcogens, and some simple C-based electrophiles. Compound **2a** also is very reactive toward alkynes, alkenes, and different heterocumulenes, and these results will be reported separately. As it will be shown below, the P atom of the phosphinidene complex **2a** is not the most nucleophilic site of the molecule, as it might have been anticipated, yet electrophile attachment at this site yields the most stable derivatives. Moreover, the particular electron distribution around this P atom, here investigated using density functional theory (DFT) methods, imposes an unusual trigonal pyramidal-like P environment in all derivatives, with the added electrophile placed in the Mo_2P plane.

RESULTS AND DISCUSSION

Synthesis and Spectroscopic Characterization of Pyramidal Phosphinidene-Bridged Complexes 2. In our preliminary study we found that compound **1** reacts with PMe_3 in toluene to form a green solution shown (by IR and NMR spectroscopy) to contain almost pure complex **2a**.¹² Although this air-sensitive product cannot be properly isolated as a crystalline solid, the crude product obtained after removal of volatiles from the above solution can be used *in situ* to study the chemical behavior of this pyramidal phosphinidene complex. For crystallization purposes, it was of interest to have at hand a related complex bearing a different phosphine ligand. We accomplished this by reacting compound **1** with dimethylphenylphosphine, which also gives the corresponding pyramidal phosphinidene derivative $[\text{Mo}_2\text{Cp}(\mu\text{-}\kappa^1:\kappa^1,\eta^5\text{-PC}_5\text{H}_4)(\eta^6\text{-HMes}^*)(\text{CO})_2(\text{PMe}_2\text{Ph})]$ (**2b**, Chart 2) almost quantitatively. This air-sensitive product could not be isolated as a crystalline solid either, but could be used *in situ* to obtain a number of derivatives.

Chart 2



Spectroscopic data for compounds **2a** and **2b** are similar to each other (Table 1), thus indicating that they share the same basic structure. The IR spectrum of these compounds displays in each case two bands with relative intensity (medium and strong, in order of decreasing frequency) indicative of a *transoid* arrangement of the CO ligands.¹³ This implies that the P atoms around the $\text{Mo}(\text{CO})_2$ fragment also should be arranged *trans* to each other, which is consistent with the low P–P coupling of ca. 25 Hz between these ligands.¹⁴ For comparison, the mononuclear complex *trans*- $[\text{WCp}(\text{CO})_2(\text{PHMes})(\text{PMe}_3)]$ ($\text{Mes} = 2,4,6\text{-C}_6\text{H}_2\text{Me}_3$) displays similar P–P coupling (39 Hz) and C–O stretches.¹⁵ We note the nuclear shielding of some 400 ppm operated on the phosphinidene P atom when changing from the trigonal mode in **1** (δ_{P} ca. 510 ppm) to the pyramidal mode in compounds **2** (δ_{P} ca. 120 ppm), stronger than anticipated. For instance, the

Table 1. Selected IR^a and ³¹P{¹H} NMR Data^b for New Compounds

compound	$\nu(\text{CO})$	$\delta(\mu\text{-P})$	$\delta(\text{PR}_3)$	J_{PP}
[Mo ₂ Cp($\mu\text{-}\kappa^1\text{:}\kappa^1\eta^5\text{-PC}_5\text{H}_4$)($\eta^6\text{-HMes}^*$)(CO) ₂] (1)	1890 (vs), 1815 (s)	509.7		
[Mo ₂ Cp($\mu\text{-}\kappa^1\text{:}\kappa^1\eta^5\text{-PC}_5\text{H}_4$)($\eta^6\text{-HMes}^*$)(CO) ₂ (PMe ₃)] (2a) ^c	1910 (m), 1842 (vs) ^d	122.0	27.3	26 ^e
[Mo ₂ Cp($\mu\text{-}\kappa^1\text{:}\kappa^1\eta^5\text{-PC}_5\text{H}_4$)($\eta^6\text{-HMes}^*$)(CO) ₂ (PMe ₂ Ph)] (2b)	1917 (m), 1843 (vs) ^d	124.0	37.1	25 ^d
[Mo ₂ Cp($\mu\text{-}\kappa^1\text{:}\kappa^1\eta^5\text{-P}(\text{BH}_3)\text{C}_5\text{H}_4$)($\eta^6\text{-HMes}^*$)(CO) ₂ (PMe ₃)] (3) ^c	1940 (m), 1863 (vs) ^d	52.3	23.7	12 ^e
[Mo ₂ Cp($\mu\text{-}\kappa^1\text{:}\kappa^1\eta^5\text{-HPC}_5\text{H}_4$)($\eta^6\text{-HMes}^*$)(CO) ₂ (PMe ₃)](BAR' ₄) (4)	1967 (m), 1890 (vs)	−31.0	18.5	24
[Mo ₂ Cp($\mu\text{-}\kappa^1\text{:}\kappa^1\eta^5\text{-HPC}_5\text{H}_4$)($\eta^6\text{-HMes}^*$)(CO) ₂ (PMe ₃)](BF ₄) (4')	1966 (m), 1888 (vs)	−29.5	18.0	24
[Mo ₂ Cp(H)($\mu\text{-}\kappa^1\text{:}\kappa^1\eta^5\text{-HPC}_5\text{H}_4$)($\eta^6\text{-HMes}^*$)(CO) ₂ (PMe ₃)](BAR' ₄) ₂ (5)	1982 (m), 1907 (vs)	48.3	14.9	22
[Mo ₂ Cp(H)($\mu\text{-}\kappa^1\text{:}\kappa^1\eta^5\text{-HPC}_5\text{H}_4$)($\eta^6\text{-HMes}^*$)(CO) ₂ (PMe ₃)](BF ₄) ₂ (5')	1977 (m), 1900 (vs)	46.5	16.5	21
[Mo ₂ Cp($\mu\text{-}\kappa^1\text{:}\kappa^1\eta^5\text{-P}(\text{S})\text{C}_5\text{H}_4$)($\eta^6\text{-HMes}^*$)(CO) ₂ (PMe ₃)] (6)	1947 (m), 1865 (vs) ^d	74.1	22.2	27 ^e
[Mo ₂ Cp($\mu\text{-}\kappa^1\text{:}\kappa^1\eta^5\text{-P}(\text{SMe})\text{C}_5\text{H}_4$)($\eta^6\text{-HMes}^*$)(CO) ₂ (PMe ₃)](BAR' ₄) (7)	1965 (m), 1889 (vs)	71.2	19.2	27
[Mo ₂ Cp($\mu\text{-}\kappa^1\text{:}\kappa^1\eta^5\text{-P}(\text{Me})\text{C}_5\text{H}_4$)($\eta^6\text{-HMes}^*$)(CO) ₂ (PMe ₃)](BAR' ₄) (8a)	1960 (m), 1882 (vs)	12.6	18.8	27
[Mo ₂ Cp($\mu\text{-}\kappa^1\text{:}\kappa^1\eta^5\text{-P}(\text{Me})\text{C}_5\text{H}_4$)($\eta^6\text{-HMes}^*$)(CO) ₂ (PMe ₂ Ph)](BAR' ₄) (8b)	1960 (m), 1883 (vs)	13.6	25.4	27
[Mo ₂ Cp($\mu\text{-}\kappa^2_{\text{P,S}}\text{:}\kappa^1_{\text{P}}\eta^5\text{-P}(\text{C}_2\text{H}_4\text{S})\text{C}_5\text{H}_4$)($\eta^6\text{-HMes}^*$)(CO) ₂] (9)	1938 (vs), 1858 (s)	88.0 ^e		

^aRecorded in dichloromethane solution, with C–O stretching bands [$\nu(\text{CO})$] in cm^{−1}. ^bRecorded in CD₂Cl₂ solution at 121.50 MHz and 298 K, with coupling constants (J_{PP}) in Hz. ^cData taken from ref 12. ^dIn toluene solution. ^eIn C₆D₆ solution.

³¹P chemical shifts of trigonal and pyramidal phosphinidene ligands in the iron complexes [Fe₃Cp₃($\mu\text{-PMe}$)($\mu\text{-PHMe}$)($\mu\text{-CO}$)₂(CO)] and [Fe₂Cp₂($\mu\text{-PMe}$)($\mu\text{-CO}$)(CO)₂] differ by some 250 ppm.¹⁶

DFT Calculations of Compound 2a. To gain more insight into the structure and chemical behavior of the pyramidal phosphinidene complex 2a we have analyzed its geometric and electronic structure using DFT methods (see the [Experimental Section](#) and [Supporting Information](#) for details). First we note that, since rotation around the P–Mo bond connecting the metallocene and Mo(CO)₂ fragments might be in principle feasible, several rotamers of this compound might exist. The two most stable ones (J and K in [Figure 1](#)) differ by only some

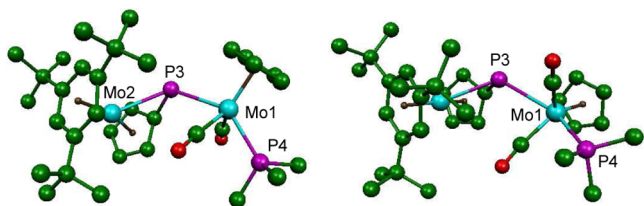


Figure 1. DFT-optimized structure of the most stable rotamers J (left) and K (right) of compound 2a, with H atoms omitted for clarity.

7 kJ/mol from each other and roughly correspond to the conformations found so far in all stable derivatives of 2a to be discussed later on. Rotamer K displays C₅ rings in an almost eclipsed arrangement, while rotamer J follows from an anticlockwise 110° rotation around the Mo–P bond in the former. These rotamers can be more precisely characterized through the corresponding P–Mo–P–Mo dihedral angles of ca. 40° (J) and −70° (K), but, apart from this, the

corresponding geometrical parameters are similar to each other ([Table 2](#)). We note that the less stable rotamer K displays a more elongated (by some 0.05 Å) Mo1–P3 bond, which suggests that the relative stability of these rotamers is mainly dictated by the steric repulsion between the metal fragments being connected by this bond, as expected. Yet the lengths of ca. 2.7 Å for such a bond in both rotamers of 2a is in any case significantly shorter than the corresponding length of 2.835 Å computed for the undetectable tricarbonyl intermediate [Mo₂Cp($\mu\text{-}\kappa^1\text{:}\kappa^1\eta^5\text{-PC}_5\text{H}_4$)($\eta^6\text{-HMes}^*$)(CO)₃] mentioned in the [Introduction](#). Since the latter difference cannot be obviously a steric effect, we therefore conclude that the presence of a poorly π acceptor phosphine ligand (compared to CO) *trans* to the Mo–P bond connecting the metal fragments in these molecules increases the strength of that bond to the point of preventing these molecules from undergoing facile Mo–P homolytic bond cleavage.

The nucleophilic character of pyramidal phosphinidene complexes expectedly arises from the presence of a lone electron pair at the P atom (usually allocated in a MO high in energy), but the presence of electron-rich metal fragments might disturb significantly this state of facts. For instance, the highest-energy MOs in the diphosphanediyl complex [Mo₂{ $\mu\text{-}\kappa^1\text{:}\kappa^1\eta^5\text{-}(\text{C}_5\text{H}_4)\text{PP}(\text{C}_5\text{H}_4)(\eta^6\text{-HMes}^*)_2$ }] (a molecule having the same metallocene fragment as compound 2a) are metal-centered orbitals, this then leading to a metal-based, rather than P-based, reactivity.¹¹ The frontier orbitals of both rotamers of 2a are similar to each other ([Figure 2](#) and [Supporting Information](#)), and indeed reveal that P-based electrons do not contribute significantly to the HOMO of the molecule, but are particularly prominent at the HOMO–2 orbital, this also having Mo–P bonding character. The HOMO of the molecule

Table 2. Geometrical Parameters for DFT-Computed Molecules^a

	ΔG^b	Mo1–P3	Mo2–P3	Mo1–P4	Mo1–P3–Mo2	P3–Mo1–P4	P4–Mo1–P3–Mo2
2a-J	0	2.697	2.710	2.474	129.6	140.2	39.5
2a-K	6.7	2.745	2.709	2.475	128.5	139.0	−69.4
4-J	3.8	2.597	2.594	2.534	144.2	137.5	41.2
4-K	0	2.584	2.598	2.537	143.2	137.7	−73.9
H-J	47.0	2.602	2.875	2.517	129.8	142.1	48.1
H-K	57.9	2.661	2.845	2.518	128.4	139.8	−80.1

^aBond lengths (Å) and angles (deg). ^bGas-phase Gibbs free energy values in kJ/mol at 298 K, relative to the most stable isomer in each case.

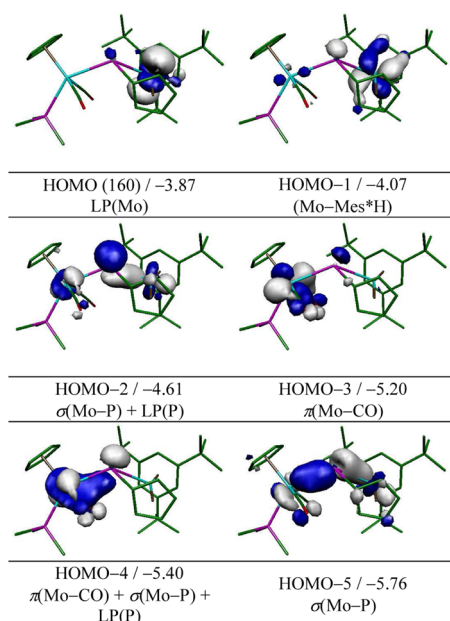


Figure 2. Selected molecular orbitals computed for rotamer J of compound **2a**, with their energies (in eV) and main bonding character indicated below. H atoms have been removed for clarity. Orbitals computed for rotamer K are similar to the ones shown here (see the Supporting Information).

instead corresponds to a lone electron pair located at the metallocene Mo atom. Moreover, atomic charges are more negative at the Mo atoms than at the P atom, which rather bears a positive charge (Mulliken charges/*e*: -0.4 (Mo1), -0.1 (Mo2), and +0.3 (P) in both rotamers).

From the above data we conclude that addition of electrophiles to compound **2a** is not particularly favored at the P site, as it might have been anticipated on the basis of its structure and preliminary reactivity. Under conditions of orbital control we would rather expect addition of electrophiles (E) at the metallocene Mo atom, following from its interaction with the HOMO of **2a**, and under conditions of charge control the result would likely be the same, after considering the coordinative saturation of the more negatively charged metal atom of the dicarbonyl fragment. As it will be shown below, however, thermodynamics seems to eventually favor the product involving the electrophile attached at the P atom. The latter would follow mainly from interaction of the electrophile with the HOMO-2 of **2a**, and we note that the lobe at P points to a direction essentially contained in the Mo₂P plane. Such directionality can be rationalized in simple terms by assuming that, in order for the P atom to more effectively bind the Mo1 and C atoms with a geometrically imposed, very acute angle Mo-P-C of ca. 60°, we may consider it to use a pure p orbital to bind the C atom, while three sp² orbitals would be used for binding to the Mo atoms and allocation of the lone electron pair (Figure 3, left). This simple bonding picture predicts Mo-P-Mo angles of 120°, not far from the computed figures of ca. 129°. In any case, this orbital directionality implies that the P environment in the corresponding product should depart strongly from a tetrahedral arrangement, with the Mo, P, and E atoms placed in the same plane (Figure 3, right), a feature already present in the structure of the borane adduct **3**,¹² which will be repeatedly found in other derivatives of **2a**, as discussed below.

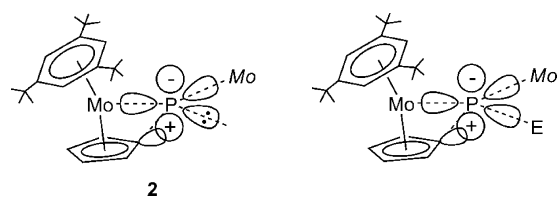
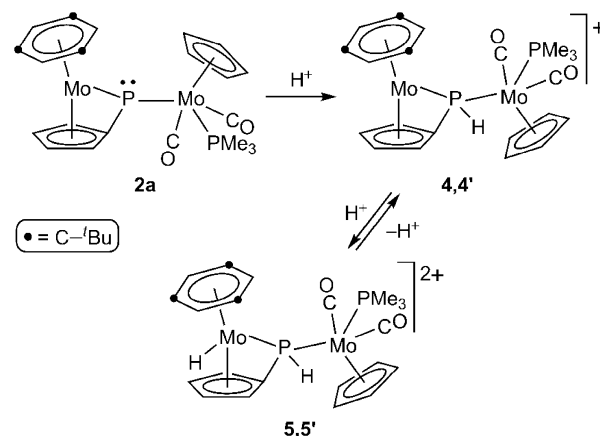


Figure 3. Simplified picture of localized orbital interactions involving the P atom in the phosphinidene-bridged complexes **2** and their derivatives following from reaction with simple electrophiles E [Mo = MoCp(CO)₂(PR₃)].

Protonation Reactions of Compound 2a. We have examined reactions of **2a** with two strong acids such as HBF₄·OEt₂ and [H(OEt₂)₂](BAR'₄), the latter having a very poorly coordinating anion [Ar' = 3,5-C₆H₃(CF₃)₂].¹⁷ The products obtained in both cases are analogous, although there are some practical differences concerning their stability or possibility of purification. Protonation with [H(OEt₂)₂](BAR'₄) could be easily carried out stepwise by using one or two equivalents of reagent: under stoichiometric conditions, protonation takes place apparently at the phosphinidene P atom, to give the phosphido-bridged monocationic [Mo₂Cp(μ-κ¹:κ¹,η⁵-HPC₅H₄)(η⁶-HMes*)(CO)₂(PMe₃)](BAR'₄) (**4**) as the unique product, which could be isolated in good yield after chromatographic workup (Scheme 2). Addition of a second

Scheme 2^a



^aAnions omitted for clarity; these are BAR'₄⁻ (for compounds **4** and **5**) or BF₄⁻ (for compounds **4'** and **5'**).

equivalent of acid involved protonation at the metallocene molybdenum site, to give the dipositive hydride complex [Mo₂Cp(H)(μ-κ¹:κ¹,η⁵-HPC₅H₄)(η⁶-HMes*)(CO)₂(PMe₃)]-(BAR'₄)₂ (**5**), a much more acidic species which is deprotonated by addition of a weak base such as tetrahydrofuran, to give back the cationic **4**. These cations could be also obtained by using HBF₄·OEt₂, although the stability of the corresponding tetrafluoroborate salts **4'** and **5'** was lower. Direct protonation of **2a** in toluene was difficult to stop at the monocation step, and rather led to the precipitation of the hydride **5'**. This product was much less stable than the borate salt **5**, and was deprotonated even by the very weakly basic diethyl ether. Actually, the tetrafluoroborate salt of the monocation **4'** was conveniently prepared by partial deprotonation of the hydride **5'** with tetrahydrofuran (see the Experimental Section).

Spectroscopic data for salts **4** and **4'** (Table 1 and Experimental Section) are similar to each other, thus indicating very weak anion–cation interactions for the tetrafluoroborate salt. The presence of a P–H bond in these cations is readily apparent in the corresponding ^1H and ^{31}P NMR spectra upon observation of a large P–H coupling of ca. 300 Hz. The phosphido ^{31}P resonance appears some 150 ppm more shielded than the phosphinidene resonance of the parent complex **2a**, as expected for a $\mu\text{-PR}_2$ group in the absence of a metal–metal bond.¹⁸ Finally, the C–O stretching bands display the same relative intensities of the parent complex **2a**, indicative of the retention of the transoid geometry at the $\text{Mo}(\text{CO})_2$ moiety, while their average frequency is some ca. 50 cm^{-1} higher, as expected from the reduced electron density at the metal sites in the cations. All of this suggests for the cations in **4** and **4'** a structure very similar to that of the parent compound **2a**, in other words, little disturbed by protonation of the phosphinidene P atom.

There are, however, two unexpected features concerning the nature of compounds **4** and **4'**. In the first place, on the basis of DFT calculations discussed above for the parent **2a**, we would have expected that addition of a proton to this neutral complex would take place at the metallocene Mo site, instead of phosphorus. Second, the protonated derivative should be in any case analogous to the borane adduct **3**, but the two-bond P–P coupling in the cations **4** is 24 Hz, thus doubling the corresponding figure in compound **3** (12 Hz). To explain these puzzling questions, we have carried out DFT calculations on the cations resulting from attachment of a proton at the P site of rotamers J and K of compound **2a** (denoted as **4-J** and **4-K**), and the hydride isomers resulting from the alternative attachment of proton at the metallocene Mo site (denoted as **H-J** and **H-K**). The optimized structures are collected in Figure 4, while their relative energy and selected geometrical parameters are collected in Table 2.

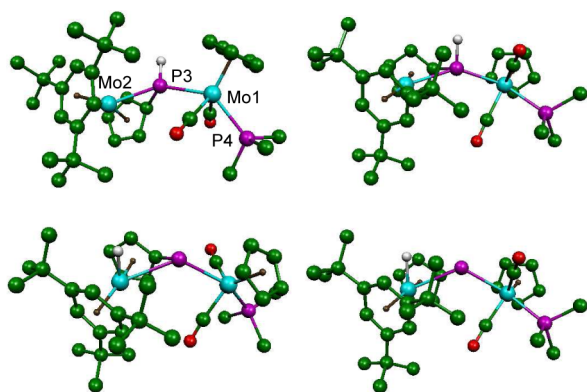


Figure 4. DFT-optimized structure of rotamers J (left) and K (right) of the cation in compound **4**, with the corresponding hydride isomers **H-J** and **H-K** shown below. Most H atoms have been omitted for clarity, and labeling is shown only for rotamer **4-J**.

First we note that the corresponding structures are little distorted with respect to those of the corresponding parent compounds, irrespective of the site of protonation (P or Mo), although energies and some bond lengths change significantly. Second, we note that the hydride isomers are significantly higher in energy than the phosphido complexes (by some 60 kJ/mol); since the corresponding Mo2–P3 lengths of ca. 2.85 Å are some 0.25 Å longer than the same lengths in the

phosphido cations **4** (ca. 2.60 Å, Table 2), it has to be concluded that the hydride cations are thermodynamically disfavored because of the strong weakening induced by the Mo-bound hydride on the adjacent Mo–P bond. Such a strong weakening effect is not observed when attaching the proton to the P atom. Third, we note that the energetic difference between rotamers remains small, with rotamer K being less stable for the hydride isomers (as computed for the parent compound **2a**) while the opposite holds for the phosphido-bridged cations **4**. Since the energetic difference between rotamers **4-J** and **4-K** is quite small, it is not surprising that replacing the proton with a different electrophile might invert the balance between rotamers. Actually, as noted above, the borane adduct **3** corresponds to a rotamer of type J, while the phosphido cation **4** is predicted to display a structure of type K. Fourth, we note that the computed P–P couplings for rotamers **4-J** and **4-K** are +4 Hz and –10 Hz respectively, with the difference of 14 Hz accurately reproducing the experimental difference of 12 Hz observed in the absolute values for this coupling in compounds **3** (12 Hz) and **4** (24 Hz). This gives support to the idea that P–P couplings are sensitive enough to the conformation of these molecules so as to serve as a diagnostic tool. Indeed, the structures of compounds **7** and **8b** to be discussed later on correspond in both cases to rotamers of type K, and the corresponding P–P couplings in solution indeed have high values (27 Hz) comparable to that of compound **4**. Finally, we note that the P–H bond in the phosphido cations **4** falls in the plane defined by the Mo and P atoms, as anticipated from the directionality exhibited by the HOMO–2 orbital of the parent compound **2a**, thus defining an unusual environment around P strongly departing from the more common tetrahedral environment.

From all the above analysis we then conclude that protonation of compound **2a** likely takes place first at the metallocene Mo site, this being followed by a fast shift of the added proton to the P site, to give the more stable phosphido-bridged derivative **4**. This is obviously facilitated by the close proximity of the hydride atom to the region occupied by the lone electron pair of the P atom ($\text{H}\cdots\text{P}$ ca. 2.80 Å). Indeed, a gas phase DFT calculation on the **H-J** to **4-K** isomerization indicates that this H-shift should take place easily in an intramolecular way (see the Supporting Information), via intermediates placed only some 20 kJ/mol above **H-J** and displaying agostic-like tricentric Mo–H–P interactions.¹⁹ The computed overall kinetic barrier is 37 kJ/mol, a very low value pointing to a very fast rearrangement in solution even at low temperature.

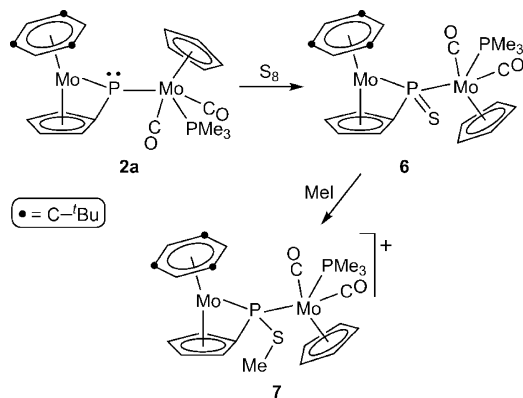
In any case, the above H-shift liberates the Mo-based electron pair at the metallocene fragment, thus enabling further protonation at this site. Indeed, analysis of the frontier orbitals of the phosphido-bridged cation in complex **4** reveals that, irrespective of the actual rotamer being considered (J or K), the HOMO of the cation is essentially localized at the metallocene Mo atom (see the Supporting Information). Thus, it is not surprising that protonation of this cation takes place again at the metallocene site, but now to give a stable hydride derivative, once the P site is already blocked. Indeed the ^1H NMR spectra of compounds **5** and **5'** display in each case a characteristically shielded hydride resonance at ca. –7 ppm coupled to phosphorus ($J_{\text{PH}} = 27\text{ Hz}$). For comparison, the structurally characterized dihydride dicationic complex $[\text{Mo}_2\{\mu\text{-}\kappa^1, \eta^5\text{:}\kappa^1, \eta^5\text{-}(\text{C}_5\text{H}_4)\text{PP}(\text{C}_5\text{H}_4)\}\text{(H)}_2(\eta^6\text{-HMes}^*)_2](\text{BF}_4)_2$ gives rise to a singlet hydride resonance at –7.10 ppm,¹¹ with the differences

in the respective P–H couplings being likely due to the presence of lone electron pairs at the P atoms in the latter complex.^{14a} In addition, we note that the C–O stretches of the cations in **5** and **5'** indicate retention of the transoid dicarbonyl structure of the parent compounds, and are only some 15 cm⁻¹ more energetic than those of **4**, which is consistent with a protonation taking place at a site remote from the Mo(CO)₂ fragment. Finally, we note that these stretches for the tetrafluoroborate salt **5'** are some 6 cm⁻¹ lower than those of **5**, which points to the presence of a moderate cation/anion pairing in solution for the former salt. The fact that one-bond P–H couplings in compounds **5** and **5'** differ significantly from each other (325 vs 334 Hz, respectively) suggests that ion pairing for these dipositive cations might be materialized in the shape of a P–H...F–BF₃ hydrogen bond like interaction.

Reactions of **2a** with Sulfur and Oxygen Sources.

Complexes of type F having pyramidal phosphinidene ligands usually react with chalcogens (E) to give the corresponding chalcogenophosphinidene-bridged (μ -P(E)R) derivatives.^{5b,20} Indeed compound **2a** is quite air-sensitive, but we could not properly isolate or characterize any of the oxo derivatives formed after on purpose exposure to air. Attempts to obtain such derivatives using milder oxygen sources such as alkene oxides failed due to lack of reaction with these reagents. Compound **2a** also reacts readily with elemental sulfur (S₈), but reaction only takes place selectively when using excess reagent and low temperatures (223 K). Under these conditions, the corresponding thiophosphinidene-bridged derivative [Mo₂Cp{ μ - κ^1 : κ^1 , η^5 -P(S)C₅H₄}(η^6 -HMes*)(CO)₂(PMe₃)] (**6**) is formed selectively (Scheme 3). The use of stoichiometric

Scheme 3



amounts of reagent or room temperature led to mixtures of **6** and up to three other compounds which could not be isolated or characterized. In addition, the use of a potentially softer source of sulfur such as ethylene sulfide led to a completely different product, to be discussed below.

Compound **6** was not very stable itself, and decomposed progressively upon attempted purification or crystallization. Fortunately, it could be indirectly stabilized via methylation, a process taking place readily upon reaction with MeI at room temperature to give the corresponding thiolatophosphido derivative, which could be conveniently isolated in good yield as the corresponding tetraarylborate salt [Mo₂Cp{ μ - κ^1 : κ^1 , η^5 -P(SMe)C₅H₄}(η^6 -HMes*)(CO)₂(PMe₃)](BAR'₄) (**7**) after anion exchange with Na(BAR'₄).

The C–O stretches of the carbonyl ligands in compounds **6** and **7** have a pattern indicative of retention of the transoid

geometry of the parent compound **2a** at the dicarbonyl fragment, and their frequencies increase expectedly in the order **2a** < **6** < **7** thus reflecting the progressive decrease of electron density at the metal centers derived from the changes operated at the bridging phosphorus ligands (μ -PR \rightarrow μ -P(S)R \rightarrow μ -P(SMe)R⁺). In contrast, the ³¹P NMR resonances of **6** and **7** appear at a very similar chemical shift of ca. 70 ppm, only moderately more shielded than the resonance of the parent compound **2a**. Moreover, this chemical shift is close to the values of ca. 100 ppm measured in the P,S:P-bridged thiophosphinidene complexes *syn*- and *anti*-[Mo₂Cp(μ - κ^2 _{P,S}: κ^1 _P, η^5 -SPC₅H₄)(η^6 -HMes*)(CO)₂].²¹ All of this indicates that the ³¹P chemical shift is a poorly sensitive structural parameter for this sort of thiophosphinidene complex. On the other hand, we note that both **6** and **7** display a relatively high P–P coupling of 27 Hz, suggestive of the prevalence in solution of a rotamer of type K, as confirmed through an X-ray study of compound **7** (Figure 5 and Table 3).

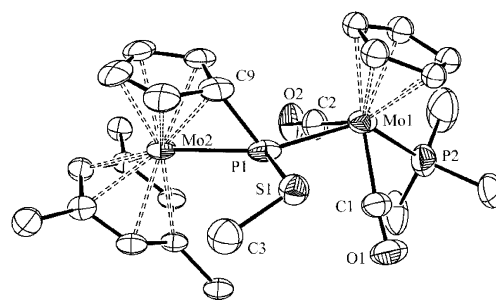


Figure 5. ORTEP diagram (30% probability) of the cation in compound **7**, with H atoms and ^tBu groups (except their C¹ atoms) omitted for clarity.

Table 3. Selected Bond Lengths (Å) and Angles (deg) for Compound **7**

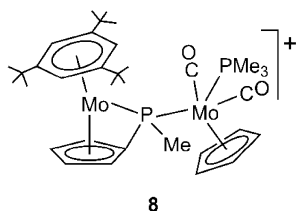
Mo1–P1	2.520(2)	Mo1–P1–Mo2	136.49(7)
Mo1–P2	2.488(3)	Mo1–P1–S1	98.2(1)
Mo1–C1	1.984(7)	Mo2–P1–S1	125.2(2)
Mo1–C2	1.976(8)	Mo2–P1–C9	58.0(2)
Mo2–P1	2.532(2)	P1–Mo1–P2	135.5(1)
Mo2–C9	2.193(6)	C1–Mo1–C2	106.5(3)
P1–S1	2.128(4)	C1–Mo1–P1	77.8(3)
P1–C9	1.783(8)	C1–Mo1–P2	75.2(3)
S1–C3	1.86(2)	C2–Mo1–P1	79.3(3)
		C2–Mo1–P2	75.4(2)
		P1–S1–C3	103.8(7)

The structure of the cation in **7** actually is comparable to the one computed for rotamer K of the phosphido-bridged cation **4**, if we just replace the H atom with the SMe group (P–Mo–P–Mo = –79.5° in **7**). Analogously, the transoid Mo(CO)₂ and the metallocene fragments are bound to the thiolatophosphido ligand so as to define a rare distorted trigonal pyramidal environment around the P1 atom, with the Mo and S atoms defining a plane that contains that P atom ($\sum(X-P-Y) = 359.9^\circ$), while the C atom of the cyclopentadienylidene ring occupies the vertex of that very distorted trigonal pyramid (Mo2–P1–C9 = 58.0(2)° rather than 90°). This P environment has been found previously in different heterometallic derivatives of compound **1** and tentatively related there to steric effects of the bulky aryl ring (HMes*) present in these molecules.²² In the case of compounds **4** and **7**, however, this

unusual geometry follows from the directionality imposed by the HOMO–2 orbital of the parent compound **2a**, as noted above. Apart from this, we note that the phosphido ligand bridges symmetrically the Mo atoms (Mo–P ca. 2.53 Å) whereas the terminal PMe_3 ligand expectedly displays a somewhat shorter length of ca. 2.49 Å. These values compare well with the figures of 2.59 and 2.54 Å computed respectively for **4-K**, if we allow for a ca. 0.05 Å overestimation of distances involving metal atoms typically obtained in common DFT calculations.²³ We finally note that only a few other complexes containing thiolatophosphido bridging ligands ($\mu\text{-P}(\text{SR})\text{R}'$) appear to have been crystallographically characterized previously,²⁴ these showing P–S lengths around ca. 2.12 Å, as found in **7** (2.128(4) Å). Other geometrical parameters of **7** are as expected and deserve no further comments.

Alkylated Derivatives of Compounds 2. Compound **2a** is easily alkylated at the P site. This can be accomplished upon reaction with a mild reagent as MeI at room temperature, a selective process allowing the isolation in good yield, after anion exchange, of the corresponding methylphosphido-bridged derivative $[\text{Mo}_2\text{Cp}\{\mu\text{-}\kappa^1:\kappa^1,\eta^5\text{-P}(\text{Me})\text{C}_5\text{H}_4\}\{\eta^6\text{-HMes}^*\}(\text{CO})_2(\text{PMe}_3)](\text{BAR}'_4)^+$ (**8a**) (Chart 3). A related

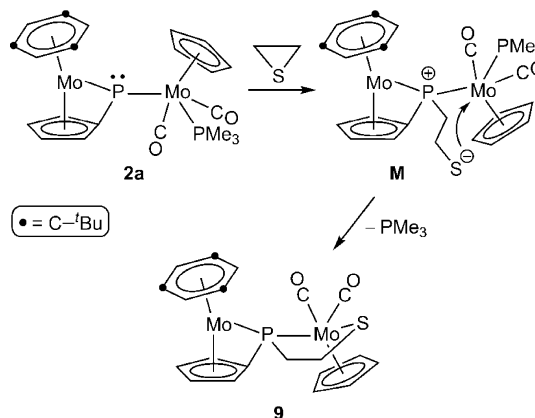
Chart 3



dimethylphenylphosphine complex **8b** could be analogously obtained from the corresponding neutral complex **2b**, and proved to yield X-ray quality crystals more easily. As noted above, we also examined the reaction of **2a** with ethylene sulfide as a possible route to the thiophosphinidene complex **6**. This reaction takes place slowly at room temperature and requires the use of excess reagent; however, it yields no significant amounts of **6**, but leads instead to the phosphido–thiolato derivative $[\text{Mo}_2\text{Cp}\{\mu\text{-}\kappa^2_{\text{P,S}}:\kappa^1_{\text{P}},\eta^5\text{-P}(\text{C}_2\text{H}_4\text{S})\text{C}_5\text{H}_4\}\{\eta^6\text{-HMes}^*\}(\text{CO})_2]$ (**9**) as major product, which can be isolated in ca. 55% yield.

The formation of **9** is likely preceded by attachment of the phosphinidene P atom at the carbon atom of the added sulfide, with opening of the C_2S ring to yield a zwitterionic intermediate **M** having increased negative charge at the S atom (Scheme 4). The latter would afterward displace the PMe_3 ligand to yield the final cyclic product, this being surely much facilitated by the presence of excess reagent reacting with the displaced phosphine ligand. In any case, it is worth stressing here the singular behavior of the pyramidal phosphinidene complex **2a** in this reaction. Although we are not aware of previous reports on reactions of phosphinidene complexes with alkene sulfides, it is interesting noting that reactions of the nucleophilic phosphinidene complex $[\text{ZrCp}_2(\text{PMe}_3^*)(\text{PMe}_3)]$ with different epoxides to yield the corresponding phosphiranes and $[\text{ZrCp}_2\text{O}]$ proceed through intermediates having PC_2OZr rings akin to the PC_2SMo ring present in **9**, with the former spontaneously evolving through cleavage of the C–O bond to yield the final products.²⁵

Scheme 4



Spectroscopic data for the methylphosphido complexes **8a,b** are very similar to each other and comparable to those of the thiolatophosphido complex **7** discussed above, with the differences expected after replacement of a SMe group with the less electron-withdrawing Me substituent (lowering of C–O stretches and ^{31}P chemical shifts), thus indicating a close structural relationship. The P–P coupling in these compounds (27 Hz) is identical to that measured for **7**, and therefore suggestive of the prevalence of conformations of type **K** in solution. Indeed, an X-ray study of complex **8b** (Figure 6 and

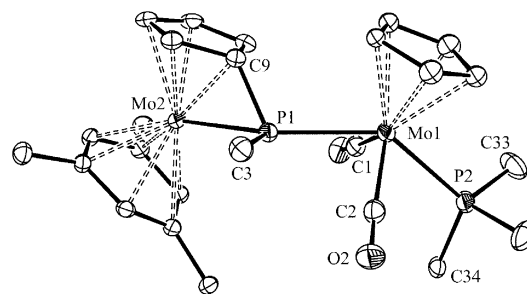


Figure 6. ORTEP diagram (30% probability) of the cation in compound **8b**, with H atoms and Ph and ^tBu groups (except their C^1 atoms) omitted for clarity.

Table 4) confirmed this arrangement in the crystal (P–Mo–P–Mo = -74.1°). Apart from the replacements Me/SMe at the P site and $\text{PMe}_3/\text{PMe}_2\text{Ph}$ at the molybdenum dicarbonyl fragment, the geometrical parameters in **8b** are very similar to those measured in **7** and therefore deserve no detailed comments. We just stress once more the unusual environment

Table 4. Selected Bond Lengths (Å) and Angles (deg) for Compound **8b**

Mo1–P1	2.532(1)	Mo1–P1–Mo2	136.86(4)
Mo1–P2	2.479(1)	Mo1–P1–C3	112.1(2)
Mo1–C1	1.986(5)	Mo2–P1–C3	111.0(2)
Mo1–C2	1.975(5)	Mo2–P1–C9	57.0(1)
Mo2–P1	2.554(1)	P1–Mo1–P2	137.94(4)
Mo2–C9	2.177(4)	C1–Mo1–C2	109.3(2)
P1–C3	1.841(5)	P1–Mo1–C1	78.4(1)
P1–C9	1.786(4)	P2–Mo1–C1	77.6(1)
P2–C33	1.831(6)	P1–Mo1–C2	78.3(1)
P2–C34	1.826(4)	P2–Mo1–C2	77.8 (1)

around phosphorus, with the Mo and C3 atoms in the same plane as P1 ($\sum(X-P-Y) = 360^\circ$) while the cyclopentadienylidene C9 atom occupies the apical position of a distorted trigonal pyramid.

The molecule of compound **9** in the crystal (Figure 7 and Table 5) is built from the usual metallocene fragment now

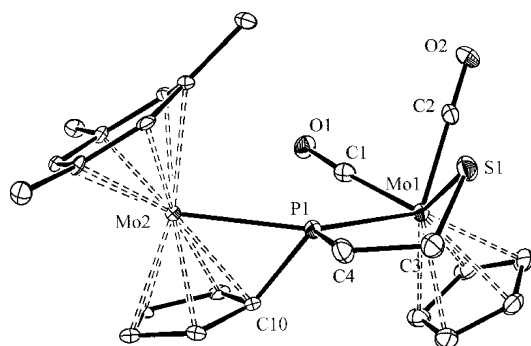


Figure 7. ORTEP diagram (30% probability) of compound **9**, with H atoms and ^tBu groups (except their C¹ atoms) omitted for clarity.

Table 5. Selected Bond Lengths (Å) and Angles (deg) for Compound **9**

Mo1–P1	2.495(2)	Mo1–P1–Mo2	137.5(1)
Mo2–P1	2.549(1)	Mo1–P1–C4	110.6(2)
Mo1–S1	2.493(2)	Mo2–P1–C4	111.3(2)
Mo1–C1	1.972(7)	Mo2–P1–C10	57.5(2)
Mo1–C2	1.954(6)	P1–Mo1–S1	74.51(5)
Mo2–C10	2.190(5)	C1–Mo1–C2	75.2(2)
P1–C4	1.886(7)	C1–Mo1–P1	79.4(2)
P1–C10	1.794(6)	C2–Mo1–P1	136.7(2)
S1–C3	1.833(7)	C1–Mo1–S1	127.6(2)
C3–C4	1.524(9)	C2–Mo1–S1	77.0(2)

attached to a cisoid Mo(CO)₂Cp fragment via the P atom of the former phosphinidene ligand, now further bound to the carbon atom of a ring-opened ethylene sulfide molecule, with the sulfur atom of the latter in turn bound to the Mo(CO)₂ fragment thus configuring a puckered PC₂SMo ring and completing a four-legged piano stool environment around the Mo1 atom. Once again, the orientation of the newly formed P1–C4 bond configures the unusual P environment found in complexes **7** and **8b**, with the Mo, P1, and C4 atoms in the same plane ($\sum(X-P-Y) = 359.4^\circ$). The interatomic distances in **9** (when comparable) are not very different from the corresponding values in the mentioned complexes and deserve no particular comments. As for the parameters involving the PC₂SMo ring, we have found just one other structurally characterized complex having a phosphido–thiolato ligand forming a comparable PC₂SM ring, the cluster [Ru₄(μ-PhPCH₂CH₂S)₂(CO)₁₀] in which, however, the bridging ligand adopts a P₂S:P₂S bridging mode, then defining a bicyclic PC₂SRu₂ framework.²⁶

Spectroscopic data in solution for **9** are consistent with the structure found in the crystal. In particular, the cisoid geometry of the Mo(CO)₂ fragment, with a C–Mo–C angle below 90° (75.2(2)° in the crystal), is denoted by the relative intensities of the C–O stretching bands (very strong and strong, in order of decreasing frequencies),¹³ and by the quite different P–C couplings of the corresponding ¹³C NMR resonances (29 and 0

Hz).¹⁴ The ¹H spectrum expectedly indicates the inequivalence of all H atoms in the PC₂SMo ring of the molecule, with one of the atoms adjacent to sulfur displaying an unusually large three-bond P–H coupling of 47 Hz. Other spectroscopic features of this compound are as expected and deserve no additional comments.

CONCLUSIONS

The title complex is stabilized by the presence of the PMe₃ ligand *trans* to the Mo–P bond of the bridging phosphinidene ligand, and it displays two nucleophilic sites, located respectively at the Mo atom of the metallocene fragment and the P atom of the pyramidal phosphinidene ligand. The former is the more favored site for attachment of simple electrophiles (E) under conditions of either orbital control or charge control, but attachment at the P atom involves fewer distortions on other bonds within the parent substrate and is then thermodynamically favored. It is thus concluded that reactions with electrophiles with little steric demands likely are initiated at the Mo site, then followed by a fast shift to the P site to yield the phosphido-bridged derivative eventually isolated in all reactions investigated. When E is a proton, this shift is computed to occur with a low kinetic barrier via intermediates displaying agostic-like tricentric Mo–H–P interactions. Permanent attachment of an electrophile at the metallocene Mo site is possible once the P site is blocked, as observed in the protonation reactions of the title compounds. The new P–E bond being formed in all the above reactions follows from interaction of the HOMO–2 orbital of the parent phosphinidene complex, and the directionality of the latter orbital drives the acceptor atom of the electrophile to the Mo₂P plane, thus configuring an unusual, trigonal pyramidal-like environment around the P atom, with the cyclopentadienylidene C atom of the former phosphinidene ligand (PC₅H₄) occupying the vertex of the pyramid. The significant steric demands of the metal fragments in these molecules pose severe restrictions on the number of conformations derived from rotation around the Mo–P bond connecting these fragments, with the most commonly favored conformation being the one involving an almost eclipsed arrangement of the C₅ rings of the molecule.

EXPERIMENTAL SECTION

General Procedures and Starting Materials. All manipulations and reactions were carried out under an argon (99.995%) atmosphere using standard Schlenk techniques. Solvents were purified according to literature procedures, and distilled prior to use.²⁷ All reagents were generally obtained from the usual commercial suppliers and used as received, unless otherwise stated. Complex **2a** was prepared *in situ* from compound **1** as described in our preliminary work,¹² and complex [Mo₂Cp₂(μ-κ¹:κ¹,η⁶-PMes*)(CO)₂],^{8b} Na(BAr'₄),²⁸ and [H(OEt)₂]₂BAr'₄²⁹ were prepared by literature procedures [Mes* = 2,4,6-C₆H₂(^tBu)₃; Ar' = 3,5-C₆H₃(CF₃)₂]. An improved preparation for the parent compound **1**^{8b} is given below. Petroleum ether refers to that fraction distilling in the range 338–343 K. Chromatographic separations were carried out using jacketed columns refrigerated by tap water (ca. 288 K) or by a closed 2-propanol circuit kept at the desired temperature with a cryostat. Commercial aluminum oxide (activity I, 70–290 mesh) was degassed under vacuum prior to use. The latter was mixed under nitrogen with the appropriate amount of water to reach activity IV. IR stretching frequencies of CO ligands were measured in solution (using CaF₂ windows), or in Nujol mulls, are referred to as ν(CO), and are given in wavenumbers (cm⁻¹). Nuclear magnetic resonance (NMR) spectra were routinely recorded at 300.13 (¹H), 121.50 (³¹P{¹H}), or 75.47 MHz (¹³C{¹H}) at 298 K in CD₂Cl₂ solution unless otherwise stated. Chemical shifts (δ) are given in ppm,

relative to internal tetramethylsilane (^1H , ^{13}C) or external 85% aqueous H_3PO_4 solutions (^{31}P). Coupling constants (J) are given in hertz.

Improved Preparation of $[\text{Mo}_2\text{Cp}(\mu\text{-}\kappa^1\text{:}\kappa^1\eta^5\text{-PC}_5\text{H}_4)(\eta^6\text{-HMes}^*)(\text{CO})_2]$ (1). Compound 1 was originally prepared through a water-catalyzed isomerization of its arylphosphinidene isomer $[\text{Mo}_2\text{Cp}_2(\mu\text{-}\kappa^1\text{:}\kappa^1\eta^6\text{-PMes}^*)(\text{CO})_2]$, a process involving a deprotonation/protonation mechanism.^{8b} The preparation of 1 can be scaled up by using a full deprotonation/protonation sequence as follows: A solution of HPF_6 (46 μL of a 60% solution in water, 0.312 mmol) was added to a dichloromethane solution (5 mL) of $[\text{Mo}_2\text{Cp}_2(\mu\text{-}\kappa^1\text{:}\kappa^1\eta^6\text{-PMes}^*)(\text{CO})_2]$ (0.200 g, 0.306 mmol), and the mixture was stirred at room temperature for 20 min. The solvent was then removed under vacuum, and the residue was dissolved in tetrahydrofuran (10 mL) and transferred using a cannula into a Schlenk tube containing solid KH (0.062 g, 1.530 mmol). This mixture was then stirred at room temperature for 40 min to give a blood-red solution. After removal of solvent, the residue was extracted with petroleum ether (3×10 mL) and the extracts were filtered using a cannula. Removal of solvent from the filtrate gave compound 1 as a red microcrystalline solid (0.190 g, 95%). Spectroscopic data for this product (Table 1) were identical to those previously reported by us for compound 1.^{8b}

Preparation of $[\text{Mo}_2\text{Cp}(\mu\text{-}\kappa^1\text{:}\kappa^1\eta^5\text{-PC}_5\text{H}_4)(\eta^6\text{-HMes}^*)(\text{CO})_2(\text{PMe}_2\text{Ph})]$ (2b). Neat PMe_2Ph (5 μL , 0.035 mmol) was added at room temperature to a red solution of complex 1 (0.020 g, 0.031 mmol) in toluene (2 mL), contained in a Schlenk tube equipped with a Young's valve, whereupon the solution turned green immediately. Removal of volatiles under vacuum gave a solid residue shown (by IR and NMR) to contain almost pure phosphinidene complex 2b. This material, however, was quite air-sensitive, and could not be isolated as a crystalline solid. IR and $^{31}\text{P}\{^1\text{H}\}$ NMR data for this complex (Table 1) were analogous to those of the PMe_3 complex 2a previously reported by us.¹²

Preparation of $[\text{Mo}_2\text{Cp}(\mu\text{-}\kappa^1\text{:}\kappa^1\eta^5\text{-HPC}_5\text{H}_4)(\eta^6\text{-HMes}^*)(\text{CO})_2(\text{PMe}_3)](\text{BAR}'_4)$ (4). Solid $[\text{H}(\text{OEt})_2]\text{BAR}'_4$ (0.031 g, 0.031 mmol) was added to a toluene solution (2 mL) of compound 2a, prepared in situ from compound 1 (0.020 g, 0.031 mmol), whereupon a green precipitate was formed. After removal of solvent under vacuum, the residue was dissolved in a minimum dichloromethane and chromatographed on alumina at 288 K. Elution with the same solvent gave a green fraction yielding, after removal of solvent, compound 4 as a green microcrystalline solid (0.031 g, 63%). Anal. Calcd for $\text{C}_{65}\text{H}_{61}\text{BF}_4\text{Mo}_2\text{O}_2\text{P}_2$: C, 48.95; H, 3.86. Found: C, 48.58; H, 3.74. ^1H NMR (300.13 MHz, CD_2Cl_2): δ 7.73 (s, br, 8H, Ar'), 7.56 (s, 4H, Ar'), 5.29 (s, 5H, Cp), 5.25, 5.18 (2m, $2 \times 1\text{H}$, C_5H_4), 4.99 (d, $^3J_{\text{PH}} = 4$, 3H, C_6H_3), 4.67, 4.54 (2m, $2 \times 1\text{H}$, C_5H_4), 3.82 [d, $^1J_{\text{PH}} = 301$, 1H, PH], 1.65 (d, $^2J_{\text{PH}} = 10$, 9H, PMe_3), 1.19 (s, 27H, 'Bu).

Preparation of $[\text{Mo}_2\text{Cp}(\mu\text{-}\kappa^1\text{:}\kappa^1\eta^5\text{-HPC}_5\text{H}_4)(\eta^6\text{-HMes}^*)(\text{CO})_2(\text{PMe}_3)](\text{BF}_4)$ (4'). Tetrahydrofuran (0.5 mL) was added to a dichloromethane solution (2 mL) of compound 5', prepared in situ from compound 1 (0.020 g, 0.031 mmol) as described below, and the mixture was stirred for 1 min to give a greenish solution. After removal of solvents, the residue was dissolved in dichloromethane and the solution was filtered through diatomaceous earth. Removal of solvent from the filtrate gave essentially pure compound 4' as a green microcrystalline powder (0.024 g, 95%). This product was quite air sensitive, and no microanalytical data were thus obtained. ^{31}P NMR (121.56 MHz, CD_2Cl_2): δ 18.0 (m, PMe_3), -29.5 (dd, $^1J_{\text{PH}} = 296$, $^2J_{\text{PP}} = 24$, $\mu\text{-PH}$). ^1H NMR (300.13 MHz, CD_2Cl_2): δ 5.34 (d, $^3J_{\text{PH}} = 1$, 5H, Cp), 5.25, 5.17 (2m, $2 \times 1\text{H}$, C_5H_4), 4.99 (d, $^3J_{\text{PH}} = 4$, 3H, C_6H_3), 4.67, 4.56 (2m, $2 \times 1\text{H}$, C_5H_4), 3.82 [d, $^1J_{\text{PH}} = 300$, 1H, $\mu\text{-PH}$], 1.70 (d, $^2J_{\text{PH}} = 9$, 9H, PMe_3), 1.20 (s, 27H, 'Bu).

Preparation of $[\text{Mo}_2\text{Cp}(\text{H})(\mu\text{-}\kappa^1\text{:}\kappa^1\eta^5\text{-HPC}_5\text{H}_4)(\eta^6\text{-HMes}^*)(\text{CO})_2(\text{PMe}_3)](\text{BAR}'_4)_2$ (5). Solid $[\text{H}(\text{OEt})_2]\text{BAR}'_4$ (0.062 g, 0.062 mmol) was added to a toluene solution (2 mL) of compound 2a, prepared in situ from compound 1 (0.020 g, 0.031 mmol), whereupon an orange precipitate was formed. After the solution was discarded, the precipitate was washed with toluene (1×2 mL) and petroleum ether (2×2 mL) and dried under vacuum to give an orange solid containing essentially pure compound 5 (0.065 g, 85%). This product could not

be further purified since it was easily deprotonated (to give compound 4) by weak bases such as tetrahydrofuran. ^{31}P NMR (121.56 MHz, CD_2Cl_2): δ 48.3 [ddd, $^1J_{\text{PH}} = 325$, $^2J_{\text{PH}} = 27$, $^2J_{\text{PP}} = 22$, $\mu\text{-PH}$], 14.9 (m, br, PMe_3). ^1H NMR (300.13 MHz, CD_2Cl_2): δ 7.73 (s, br, 16H, Ar'), 7.57 (s, 8H, Ar'), 6.05 (s, 3H, C_6H_3), 6.00, 5.66, 5.63 (3m, $3 \times 1\text{H}$, C_5H_4), 5.37 (s, 5H, Cp), 5.02 (m, 1H, C_5H_4), 4.86 [d, br, $^1J_{\text{PH}} = 325$, 1H, $\mu\text{-PH}$], 1.69 (d, $^2J_{\text{PH}} = 10$, 9H, PMe_3), 1.25 (s, 27H, 'Bu), -7.79 (d, $^2J_{\text{PH}} = 27$, 1H, MoH). $^1\text{H}\{^{31}\text{P}\}$ NMR (300.13 MHz, CD_2Cl_2): δ 7.73 (s, 16H, Ar'), 7.57 (s, 8H, Ar'), 6.05 (s, 3H, C_6H_3), 6.00, 5.66, 5.63 (3m, $3 \times 1\text{H}$, C_5H_4), 5.37 (s, 5H, Cp), 5.02 (m, 1H, C_5H_4), 4.86 [s, 1H, $\mu\text{-PH}$], 1.69 (s, 9H, PMe_3), 1.25 (s, 27H, 'Bu), -7.79 (s, 1H, MoH).

Preparation of $[\text{Mo}_2\text{Cp}(\text{H})(\mu\text{-}\kappa^1\text{:}\kappa^1\eta^5\text{-HPC}_5\text{H}_4)(\eta^6\text{-HMes}^*)(\text{CO})_2(\text{PMe}_3)](\text{BF}_4)_2$ (5'). Neat $\text{HBF}_4 \cdot \text{OEt}_2$ (10 μL , 0.073 mmol) was added to a toluene solution (2 mL) of compound 2a, prepared in situ from compound 1 (0.020 g, 0.031 mmol), whereupon an orange precipitate was formed. After the solution was discarded, the precipitate was washed with toluene (2×2 mL) and dried under vacuum to give an orange solid containing essentially pure compound 5' (0.025 g, 90%). This product, however, could not be further purified since it was easily deprotonated (to give compound 4') by even very weak bases such as diethyl ether. ^{31}P NMR (121.56 MHz, CD_2Cl_2): δ 46.5 [ddd, $^1J_{\text{PH}} = 344$, $^2J_{\text{PH}} = 27$, $^2J_{\text{PP}} = 21$, $\mu\text{-PH}$], 16.5 (m, br, PMe_3). ^1H NMR (300.13 MHz, CD_2Cl_2): δ 6.22 (m, 1H, C_5H_4), 6.10 (s, 3H, C_6H_3), 5.92, 5.77 (2m, $2 \times 1\text{H}$, C_5H_4), 5.54 (s, 5H, Cp), 5.42 (m, 1H, C_5H_4), 5.19 [d, $^1J_{\text{PH}} = 344$, $^3J_{\text{PH}} = 2$ Hz, 1H, $\mu\text{-PH}$], 1.74 (d, $^2J_{\text{PH}} = 9$, 9H, PMe_3), 1.31 (s, 27H, 'Bu), -7.67 (d, $^2J_{\text{PH}} = 27$, 1H, MoH). $^1\text{H}\{^{31}\text{P}\}$ NMR (300.13 MHz, CD_2Cl_2): δ 6.22 (m, 1H, C_5H_4), 6.10 (s, 3H, C_6H_3), 5.92, 5.77 (2m, $2 \times 1\text{H}$, C_5H_4), 5.54 (s, 5H, Cp), 5.42 (m, 1H, C_5H_4), 5.19 [s, 1H, $\mu\text{-PH}$], 1.74 (s, 9H, PMe_3), 1.31 (s, 27H, 'Bu), -7.67 (s, 1H, MoH).

Preparation of $[\text{Mo}_2\text{Cp}(\mu\text{-}\kappa^1\text{:}\kappa^1\eta^5\text{-P}(\text{S})\text{C}_5\text{H}_4)(\eta^6\text{-HMes}^*)(\text{CO})_2(\text{PMe}_3)]$ (6). A solution of S_8 in toluene (1.5 mL of a 0.0078 M solution, 0.012 mmol) was added to a toluene solution (2 mL) of compound 2a, prepared in situ from compound 1 (0.020 g, 0.031 mmol) and previously cooled at 223 K, and the mixture was stirred for 5 min to give a dark green solution, then allowed to reach room temperature and filtered using a cannula. After removal of solvent from the filtrate, the residue was washed with petroleum ether (2×5 mL) and dried under vacuum to give essentially pure compound 6 as a yellow-brown microcrystalline solid (0.020 g, 85%). This product was quite air sensitive and could not be further purified; therefore no microanalytical data were obtained for this material. ^1H NMR (300.13 MHz, C_6D_6): δ 6.93, 5.52, 5.11 (3m, $3 \times 1\text{H}$, C_5H_4), 4.92 (s, 5H, Cp), 4.84 (s, 3H, C_6H_3), 4.33 (m, 1H, C_5H_4), 1.31 (s, 27H, 'Bu), 0.81 (d, $^2J_{\text{PH}} = 9$, 9H, PMe_3).

Preparation of $[\text{Mo}_2\text{Cp}(\mu\text{-}\kappa^1\text{:}\kappa^1\eta^5\text{-P}(\text{SMe})\text{C}_5\text{H}_4)(\eta^6\text{-HMes}^*)(\text{CO})_2(\text{PMe}_3)](\text{BAR}'_4)$ (7). Neat MeI (10 mL, 0.160 mmol) was added to a crude toluene solution of compound 6, prepared as described above (ca. 0.031 mmol), and the mixture was stirred at room temperature for 5 min. After removal of volatiles, the residue was dissolved in dichloromethane (5 mL), solid $\text{Na}(\text{BAR}'_4)$ (0.027 g, 0.031 mmol) was added, and the mixture was stirred for 10 min. After removal of solvent under vacuum, the residue was extracted with dichloromethane/petroleum ether (1/1) and the extracts were chromatographed on alumina at 258 K. Elution with the same solvent mixture gave a green fraction yielding, after removal of solvents, compound 7 as a green microcrystalline solid (0.038 g, 75%). The crystals used in the X-ray study were grown by the slow diffusion of layers of diethyl ether and petroleum ether into a concentrated dichloromethane solution of the complex at 253 K. Anal. Calcd for $\text{C}_{66}\text{H}_{63}\text{BF}_4\text{Mo}_2\text{O}_2\text{P}_2\text{S}$: C, 48.31; H, 3.87; S, 1.95. Found: C, 48.04; H, 3.65; S, 1.70. ^1H NMR (400.13 MHz, CD_2Cl_2): δ 7.72 (s, br, 8H, Ar'), 7.56 (s, 4H, Ar'), 5.35 (d, $^3J_{\text{HP}} = 2$, 5H, Cp), 5.22, 5.18, 4.98 (3m, $3 \times 1\text{H}$, C_5H_4), 4.94 (d, $^3J_{\text{HP}} = 4$, 3H, C_6H_3), 4.16 (m, 1H, C_5H_4), 2.31 (d, $^3J_{\text{HP}} = 9$, 3H, Me), 1.66 (d, $^2J_{\text{HP}} = 10$, 9H, PMe_3), 1.21 (s, 27H, 'Bu). $^{13}\text{C}\{^1\text{H}\}$ NMR (100.63 MHz, CD_2Cl_2): δ 235.3, 231.5 (2m, MoCO), 162.2 [q, $^1J_{\text{CB}} = 50$, $\text{C}^1(\text{Ar}')$], 135.2 [s, $\text{C}^2(\text{Ar}')$], 129.3 [q, $^2J_{\text{CF}} = 32$, $\text{C}^3(\text{Ar}')$], 125.1 [q, $^1J_{\text{CF}} = 272$, CF_3], 117.9 [s, $\text{C}^4(\text{Ar}')$], 114.5 [s, $\text{C}(\text{C}_6\text{H}_3)$], 95.0 [s, br, $\text{C}(\text{C}_5\text{H}_4)$], 93.4 (s, Cp), 90.5 [s, br,

CH(C₅H₄), 88.5, 86.9 [2s, CH(C₅H₄)], 81.7 [s, br, CH(C₅H₄)], 73.3 [s, CH(C₆H₃)], 35.6 [s, C¹(^tBu)], 31.3 [s, C²(^tBu)], 24.4 (s, br, SMe), 20.1 [d, ¹J_{CP} = 34, PMe₃].

Preparation of [Mo₂Cp(μ-κ¹:κ¹, η⁵-P(Me)C₅H₄)(η⁶-HMes*)(CO)₂(PMe₃)](BAR'₄) (8a). Neat MeI (10 mL, 0.160 mmol) was added to a toluene solution (2 mL) of compound 2a, prepared in situ from compound 1 (0.020 g, 0.031 mmol), and the mixture was stirred for 2 min, whereupon a green precipitate was formed. After removal of volatiles, the residue was dissolved in dichloromethane (5 mL), solid Na(BAR'₄) (0.027 g, 0.031 mmol) was added, and the mixture was stirred for 10 min. The solvent was then removed, the residue was extracted with dichloromethane/petroleum ether (1/2), and the extracts were chromatographed on alumina at 258 K. Elution with the same solvent mixture gave a green fraction yielding, after removal of solvents, compound 8a as a green microcrystalline solid (0.045 g, 90%). Anal. Calcd for C₆₆H₆₃BF₂₄Mo₂O₂P₂: C, 49.27; H, 3.95. Found: C, 48.94; H, 3.65. ¹H NMR (400.13 MHz, CD₂Cl₂): δ 7.74 (s, br, 8H, Ar'), 7.57 (s, 4H, Ar'), 5.26 (s, 5H, Cp), 5.22, 5.13, 4.92 (3m, 3 × 1H, C₅H₄), 4.82 (d, ³J_{HP} = 5, 3H, C₆H₃), 4.26 (m, 1H, C₅H₄), 1.82 (d, ²J_{HP} = 8, 3H, PMe), 1.62 (d, ²J_{HP} = 9, 9H, PMe₃), 1.18 (s, 27H, ^tBu). ¹³C{¹H} NMR (100.63 MHz, CD₂Cl₂): δ 234.5 (m, 2 MoCO), 162.2 [q, ¹J_{CB} = 50, C¹(Ar')], 135.3 [s, C²(Ar')], 129.3 [q, ²J_{CF} = 32, C³(Ar')], 125.1 [q, ¹J_{CF} = 272, CF₃], 117.9 [s, C⁴(Ar')], 113.7 [s, C(C₆H₃)], 95.9 [d, ¹J_{CP} = 16, C(C₅H₄)], 92.9 (s, Cp), 90.8 [d, ²J_{CP} = 9, CH(C₅H₄)], 88.1 [d, ²J_{CP} = 4, CH(C₅H₄)], 83.9 [s, CH(C₅H₄)], 83.6 [d, ²J_{CP} = 14, CH(C₅H₄)], 72.3 [s, CH(C₆H₃)], 35.2 [s, C¹(^tBu)], 31.2 [s, C²(^tBu)], 22.8 (s, br, PMe), 20.3 [d, ¹J_{CP} = 34, PMe₃].

Preparation of [Mo₂Cp(μ-κ¹:κ¹, η⁵-P(Me)C₅H₄)(η⁶-HMes*)(CO)₂(PMe₂Ph)](BAR'₄) (8b). The procedure is identical to that described above for 8a, but starting with complex 2b (ca. 0.031 mmol). After similar workup, compound 8b was isolated as a green microcrystalline solid (0.039 g, 75%). The crystals used in the X-ray study were grown by the slow diffusion of layers of diethyl ether and petroleum ether into a concentrated dichloromethane solution of the complex at 253 K. Anal. Calcd for C₇₁H₆₅BF₂₄Mo₂O₂P₂: C, 51.04; H, 3.92. Found: C, 50.75; H, 3.73. ¹H NMR (400.13 MHz, CD₂Cl₂): δ 7.73 (s, br, 8H, Ar'), 7.56 (s, 4H, Ar'), 7.65–7.50 (m, 5H, Ph), 5.23, 5.14 (2m, 2 × 1H, C₅H₄), 5.08 (s, 5H, Cp), 4.92 (m, 1H, C₅H₄), 4.83 (d, ³J_{HP} = 5, 3H, C₆H₃), 4.27 (m, 1H, C₅H₄), 1.97, 1.95 (2d, ²J_{HP} = 9, 2 × 3H, PPhMe₂), 1.84 (d, ²J_{HP} = 8, 3H, PMe), 1.19 (s, 27H, ^tBu).

Preparation of [Mo₂Cp(μ-κ²:κ¹:κ¹, η⁵-P(C₂H₅)₂C₅H₄)(η⁶-HMes*)(CO)₂] (9). Ethylene sulfide (12 μL, 0.186 mmol) was added to a toluene solution (2 mL) of compound 2a, prepared in situ from compound 1 (0.040 g, 0.062 mmol), and the mixture was stirred for 60 min to give a rose solution. After removal of volatiles under vacuum, the residue was extracted with dichloromethane/petroleum ether (1/3) and the extracts were chromatographed on alumina at 288 K. Elution with the same solvent mixture gave a rose fraction yielding, after removal of solvents, compound 9 as a rose microcrystalline solid (0.025 g, 56%). The crystals used in the X-ray study were grown by the slow diffusion of layers of diethyl ether and petroleum ether into a concentrated toluene solution of the complex at 253 K. Anal. Calcd for C₃₂H₄₃Mo₂O₂PS: C, 53.78; H, 6.07; S, 4.49. Found: C, 53.34; H, 5.85; S, 4.26. ¹H NMR (300.09 MHz, C₆D₆): δ 5.09 (s, 5H, Cp), 4.88, 4.74 (2m, 2 × 1H, C₅H₄), 4.66 (d, ³J_{PH} = 3, 3H, C₆H₃), 4.59, 4.30 (2m, 2 × 1H, C₅H₄), 3.09 [dddd, ³J_{PH} = 47, ²J_{HH} = 12, 6, 2, 1H, SCH₂], 2.01, 1.80 [2m, 2 × 1H, PCH₂], 1.54 [m, 1H, SCH₂], 1.12 (s, 27H, ^tBu). ¹³C{¹H} NMR (100.63 MHz, C₆D₆): δ 254.5 (d, ²J_{CP} = 29, MoCO), 241.3 (s, MoCO), 111.3 [s, br, C(C₆H₃)], 97.6 [d, ¹J_{CP} = 26, C(C₅H₄)], 93.6 (s, Cp), 90.7, 85.9, 84.8, 84.7 [4s, CH(C₅H₄)], 70.5 [s, CH(C₆H₃)], 37.4 [d, ¹J_{CP} = 13, PCH₂], 35.1 [d, ²J_{CP} = 10, SCH₂], 35.0 [s, C¹(^tBu)], 31.4 [s, C²(^tBu)].

X-ray Structure Determination of Compounds 7, 8b, and 9.

Data collection for these compounds was performed at low temperature on an Oxford Diffraction Xcalibur Nova single crystal diffractometer, using Cu Kα radiation. Images were collected at a 62 mm (63 mm for 9) fixed crystal–detector distance, using the oscillation method, with 1° oscillation and variable exposure time per image. Data collection strategy was calculated with the program *CrysAlis Pro CCD*,³⁰ and data reduction and cell refinement was

performed with the program *CrysAlis Pro RED*.³⁰ An empirical absorption correction was applied using the SCALE3 ABSPACK algorithm as implemented in the latter program. Using the program suite WINGX,³¹ the structures were solved by Patterson interpretation and phase expansion (7 and 8b), or by direct methods (9), and were refined with full-matrix least-squares on *F*² using SHELXL97 or SHELXL2014.³² In general, all positional parameters and temperature factors for non-H atoms were refined anisotropically except for atoms involved in disorder, which had to be refined isotropically to prevent their temperature factors from becoming non-positive definite, and all hydrogen atoms were geometrically placed and refined using a riding model. For compound 7, the SMe group and the cyclopentadienyl ligand in the cation, as well as one CF₃ group of the anion, were found to be disordered over two sites, satisfactorily modeled with 0.5 occupancies; less pronounced disorders were also present for the ^tBu groups in the cation and other CF₃ groups in the anion, but these were not modeled. Compound 8b was found to crystallize with half a molecule of diethyl ether; in addition, three CF₃ groups and the cyclopentadienyl ligand were found to be disordered over two positions and satisfactorily modeled with 0.5 occupancies. Crystallographic data and structure refinement details for all these compounds are collected in Table S1.

Computational Details. All DFT calculations were carried out using the GAUSSIAN03 package,³³ in which the hybrid method B3LYP was used with the Becke three-parameter exchange functional,³⁴ and the Lee–Yang–Parr correlation functional.³⁵ Effective core potentials and their associated double-ζ LANL2DZ basis set were used for the Mo atoms.³⁶ The light elements (P, O, C, and H) were described with the 6-31G* basis.³⁷ Geometry optimizations were performed under no symmetry restrictions, using initial coordinates derived from the X-ray data of compounds 3 and 7. Frequency analyses were performed for all the stationary points to ensure that a minimum structure with no imaginary frequencies was achieved. Molecular orbitals and vibrational modes were visualized using the MOLEKEL program.³⁸ NMR shielding contributions and coupling constants were calculated using the gauge-including atomic orbitals (GIAO) method,³⁹ in combination with the LANL2DZ basis set for the Mo atoms and the IGLO-III basis set of Kutzelnigg and co-workers for the remaining atoms.⁴⁰ Transition states were optimized using the synchronous transit-guided quasi-Newton (STQN) method as implemented in Gaussian and were identified by the presence of one imaginary frequency. Their connectivity was corroborated either by visual inspection of the corresponding vibration or by IRC calculations.

■ ASSOCIATED CONTENT

Supporting Information

The Supporting Information is available free of charge on the ACS Publications website at DOI: 10.1021/acs.inorgchem.5b01527.

Crystal data and DFT-computed data (PDF)

Full crystallographic data for 7, 8b, and 9 (CCDC 1405861–1405863) (CIF)

■ AUTHOR INFORMATION

Corresponding Authors

*E-mail: garciavdaniel@uniovi.es.

*E-mail: mara@uniovi.es.

Notes

The authors declare no competing financial interest.

■ ACKNOWLEDGMENTS

We thank the DGI of Spain for financial support (Project CTQ2012-33187) and the X-ray unit of the Universidad de Oviedo for acquisition of diffraction data.

REFERENCES

- (1) Reviews: (a) Protasiewicz, J. D. *Eur. J. Inorg. Chem.* **2012**, 4539. (b) Aktas, H.; Slootweg, J. C.; Lammertsma, K. *Angew. Chem., Int. Ed.* **2010**, *49*, 2102. (c) Kollár, L.; Keglevich, G. *Chem. Rev.* **2010**, *110*, 4257. (d) Waterman, R. *Dalton Trans.* **2009**, 18. (e) Mathey, F. *Dalton Trans.* **2007**, 1861. (f) Lammertsma, K. *Top. Curr. Chem.* **2003**, *229*, 95. (g) Streubel, R. *Top. Curr. Chem.* **2003**, *223*, 91. (h) Mathey, F. *Angew. Chem., Int. Ed.* **2003**, *42*, 1578. (i) Lammertsma, K.; Vlaar, M. J. M. *Eur. J. Org. Chem.* **2002**, 1127. (j) Mathey, F.; Huy, N. H. T.; Marinetti, A. *Helv. Chim. Acta* **2001**, *84*, 2938. (k) Stephan, D. W. *Angew. Chem., Int. Ed.* **2000**, *39*, 314. (l) Shah, S.; Protasiewicz, J. D. *Coord. Chem. Rev.* **2000**, *210*, 181.
- (2) Dillon, K. B.; Mathey, F.; Nixon, J. F. *Phosphorus: The Carbon Copy*; Wiley: New York, 1998.
- (3) Type D complexes: (a) Alvarez, M. A.; Amor, I.; García, M. E.; García-Vivó, D.; Ruiz, M. A.; Sáez, D.; Hamidov, H.; Jeffery, J. C. *Inorg. Chim. Acta* **2015**, *424*, 103 and references therein. (b) Hüttner, G.; Evertz, K. *Acc. Chem. Res.* **1986**, *19*, 406.
- (4) Type E complexes: Alvarez, M. A.; Amor, I.; García, M. E.; García-Vivó, D.; Ruiz, M. A.; Suárez, J. *Organometallics* **2012**, *31*, 2749 and references therein.
- (5) Type F complexes: (a) Alvarez, M. A.; García, M. E.; González, R.; Ruiz, M. A. *Organometallics* **2013**, *32*, 4601. (b) Alvarez, M. A.; García, M. E.; González, R.; Ruiz, M. A. *Dalton Trans.* **2012**, *41*, 14498 and references therein.
- (6) For recent work from other groups on binuclear phosphinidene-bridged complexes, see: (a) Seidl, M.; Kuntz, C.; Bodensteiner, M.; Timoshkin, A. Y.; Scheer, M. *Angew. Chem., Int. Ed.* **2015**, *54*, 2771. (b) Zhou, J.; Li, T.; Maron, L.; Leng, X.; Chen, Y. *Organometallics* **2015**, *34*, 470. (c) Lv, Y.; Kefalidis, C. E.; Zhou, J.; Maron, L.; Leng, X.; Chen, Y. *J. Am. Chem. Soc.* **2013**, *135*, 14784. (d) Stubenhofer, M.; Lassandro, G.; Balázs, G.; Timoshkin, A. Y.; Scheer, M. *Chem. Commun.* **2012**, 48, 7262. (e) Grubba, R.; Wisniewska, A.; Baranowska, K.; Matern, E.; Pikies, J. *Dalton Trans.* **2011**, *40*, 2017. (f) Scheer, M.; Kuntz, C.; Stubenhofer, M.; Zabel, M.; Timoshkin, A. Y. *Angew. Chem., Int. Ed.* **2010**, *49*, 188. (g) Stubenhofer, M.; Kuntz, C.; Balázs, G.; Zabel, M.; Scheer, M. *Chem. Commun.* **2009**, 1745. (h) Scheer, M.; Himmel, D.; Kuntz, C.; Zhan, S.; Leiner, E. *Chem. - Eur. J.* **2008**, *14*, 9020. (i) Cui, P.; Chen, Y.; Xu, X.; Sun, J. *Chem. Commun.* **2008**, 5547. (j) Masuda, J. D.; Jantunen, K. C.; Ozerov, O. V.; Noonan, J. T.; Gates, D. P.; Scott, B. L.; Kiplinger, J. L. *J. Am. Chem. Soc.* **2008**, *130*, 2408. (k) Graham, T. W.; Udachin, K. A.; Carty, A. J. *Inorg. Chim. Acta* **2007**, *360*, 1376. (l) Graham, T. W.; Udachin, K. A.; Carty, A. J. *Chem. Commun.* **2006**, 2699.
- (7) Cowley, A. H.; Giolando, D. M.; Nunn, C. M.; Pakulski, M.; Westmoreland, D.; Norman, N. C. *J. Chem. Soc., Dalton Trans.* **1988**, 2127.
- (8) (a) García, M. E.; Riera, V.; Ruiz, M. A.; Sáez, D.; Vaissermann, J.; Jeffery, J. C. *J. Am. Chem. Soc.* **2002**, *124*, 14304. (b) Amor, I.; García, M. E.; Ruiz, M. A.; Sáez, D.; Hamidov, H.; Jeffery, J. C. *Organometallics* **2006**, *25*, 4857. (9) Grubba, R.; Baranowska, K.; Gudat, D.; Pikies, J. *Organometallics* **2011**, *30*, 6655. (10) Alvarez, M. A.; García, M. E.; Ruiz, M. A.; Suárez, J. *Angew. Chem., Int. Ed.* **2011**, *50*, 6383. (11) Alvarez, M. A.; García, M. E.; García-Vivó, D.; Ramos, A.; Ruiz, M. A.; Suárez, J. *Inorg. Chem.* **2012**, *51*, 34. (12) Albuérne, I. G.; Alvarez, M. A.; García, M. E.; García-Vivó, D.; Ruiz, M. A. *Organometallics* **2013**, *32*, 6178. (13) Braterman, P. S. *Metal Carbonyl Spectra*; Academic Press: London, U.K., 1975. (14) A general trend established for $^2J_{XY}$ in complexes of the type $[MCpXYL_2]$ is that $|J_{cis}| > |J_{trans}|$. See, for instance: (a) Jameson, C. J. In *Phosphorus-31 NMR Spectroscopy in Stereochemical Analysis*; Verkade, J. G., Quin, L. D., Eds.; VCH: Deerfield Beach, FL, 1987; Chapter 6. (b) Wrackmeyer, B.; Alt, H. G.; Maisel, H. E. *J. Organomet. Chem.* **1990**, *399*, 125. (15) Malisch, W.; Hirth, U. A.; Bright, T. A.; Káb, H.; Ertel, T. S.; Hüeckmann, S.; Bertagnolli, H. *Angew. Chem., Int. Ed. Engl.* **1992**, *31*, 1525. (16) Alvarez, M. A.; García, M. E.; González, R.; Ramos, A.; Ruiz, M. A. *Organometallics* **2011**, *30*, 1102. (17) (a) Krossing, I.; Raabe, I. *Angew. Chem., Int. Ed.* **2004**, *43*, 2066. (b) Strauss, S. H. *Chem. Rev.* **1993**, *93*, 927. (c) Seppelt, K. *Angew. Chem., Int. Ed. Engl.* **1993**, *32*, 1025. (18) Carty, A. J.; MacLaughlin, S. A.; Nucciarone, D. In *Phosphorus-31 NMR Spectroscopy in Stereochemical Analysis*; Verkade, J. G., Quin, L. D., Eds.; VCH: Deerfield Beach, FL, 1987; Chapter 16. (19) Alvarez, M. A.; García, M. E.; Martínez, M. E.; Ramos, A.; Ruiz, M. A.; Sáez, D.; Vaissermann, J. *Inorg. Chem.* **2006**, *45*, 6965 and references therein. (20) Kourkine, I. V.; Glueck, D. S. *Inorg. Chem.* **1997**, *36*, 5160. (21) Alvarez, B.; Alvarez, M. A.; Amor, I.; García, M. E.; García-Vivó, D.; Ruiz, M. A.; Suárez, J. *Inorg. Chem.* **2012**, *51*, 7810. (22) Alvarez, M. A.; Amor, I.; García, M. E.; García-Vivó, D.; Ruiz, M. A.; Suárez, J. *Organometallics* **2010**, *29*, 4384. (23) (a) Koch, W.; Holthausen, M. C. *A Chemist's Guide to Density Functional Theory*, 2nd ed.; Wiley-VCH: Weinheim, 2002. (b) Cramer, C. J. *Essentials of Computational Chemistry*, 2nd ed.; Wiley: Chichester, U.K., 2004. (24) (a) Evertz, K.; Huttner, G. *Chem. Ber.* **1987**, *120*, 937. (b) Lindner, E.; Auch, K.; Hiller, W.; Fawzi, R. *Z. Naturforsch., B: J. Chem. Sci.* **1987**, *42*, 454. (c) Evertz, K.; Huttner, G. *Chem. Ber.* **1988**, *121*, 143. (25) Breen, T. L.; Stephan, D. W. *J. Am. Chem. Soc.* **1995**, *117*, 11914. (26) Byrne, L. T.; Hondow, N. S.; Koutsantonis, G. A.; Skelton, B. W.; Torabi, A. A.; White, A. L.; Wild, S. B. *J. Organomet. Chem.* **2008**, *693*, 1738. (27) Armarego, W. L. F.; Chai, C. C. C. *Purification of Laboratory Chemicals*, 5th ed.; Butterworth-Heinemann: Oxford, U.K., 2003. (28) Yakelis, N. A.; Bergman, R. G. *Organometallics* **2005**, *24*, 3579. (29) (a) Nishida, H.; Takada, N.; Yoshimura, M.; Sonoda, T.; Kobayashi, H. *Bull. Chem. Soc. Jpn.* **1984**, *57*, 2600. (b) Brookhart, M.; Grant, B.; Volpe, A. F., Jr. *Organometallics* **1992**, *11*, 3920. (30) *CrysAlis Pro*; Oxford Diffraction Ltd.: Oxford, U. K., 2006. (31) Farrugia, L. J. *J. Appl. Crystallogr.* **1999**, *32*, 837. (32) Sheldrick, G. M. *Acta Crystallogr., Sect. A: Found. Crystallogr.* **2008**, *A64*, 112. (33) Frisch, M. J.; et al. *Gaussian 03, Revision B.02* (see [Supporting Information](#)). (34) Becke, A. D. *J. Chem. Phys.* **1993**, *98*, 5648. (35) Lee, C.; Yang, W.; Parr, R. G. *Phys. Rev. B: Condens. Matter Mater. Phys.* **1988**, *37*, 785. (36) Hay, P. J.; Wadt, W. R. *J. Chem. Phys.* **1985**, *82*, 299. (37) (a) Hariharan, P. C.; Pople, J. A. *Theor. Chim. Acta* **1973**, *28*, 213. (b) Petersson, G. A.; Al-Laham, M. A. *J. Chem. Phys.* **1991**, *94*, 6081. (c) Petersson, G. A.; Bennett, A.; Tensfeldt, T. G.; Al-Laham, M. A.; Shirley, W. A.; Mantzaris, J. *J. Chem. Phys.* **1988**, *89*, 2193. (38) Portmann, S.; Luthi, H. P. *Chimia* **2000**, *54*, 766. (39) Wolinski, K.; Hinton, J. F.; Pulay, P. *J. Am. Chem. Soc.* **1990**, *112*, 8251. (40) Kutzelnigg, W.; Fleischer, U.; Schindler, M. *NMR* **1990**, *23*, 165.